ADVANCING EARTH AND SPACE SCIENCES

Geophysical Research Letters

RESEARCH LETTER
10.1029/2024GL109410

# Evidences of Permafrost Signatures in the Planform Shape of Arctic Meandering Streams

**Niccolò Ragno[1], Riccardo Bonanomi[2], Marta Crivellaro[2], and Marco Tubino[1]**

[1]Department of Civil, Environmental, and Mechanical Engineering, University of Trento, Trento, Italy, [2]Center Agriculture Food Environment, University of Trento, Trento, Italy

**Key Points:**

- Permafrost is found to leave a morphological signature in the spatio-temporal signal of channel width at the bend scale
- Permafrost meander bends show larger amplitude of width oscillations and widen as sinuosity increases
- Bend curvature as a standalone indicator does not provide evidence of any significant permafrost-fingerprint

**Supporting Information:**

Supporting Information may be found in the online version of this article.

**Correspondence to:**

N. Ragno,
niccolo.ragno@unitn.it

**Citation:**

Ragno, N., Bonanomi, R., Crivellaro, M., & Tubino, M. (2024). Evidences of permafrost signatures in the planform shape of Arctic meandering streams. *Geophysical Research Letters*, *51*, e2024GL109410. https://doi.org/10.1029/2024GL109410

Received 21 MAR 2024
Accepted 19 JUN 2024

**Abstract** We investigate whether geomorphic signatures of permafrost are embedded in planforms of river meanders, and we inquire as to how physical factors unique to permafrost environments are able to affect their dynamics. By exploiting satellite imagery, a data set of 19 freely-meandering Arctic rivers is compared against an independent data set of 23 freely-meandering streams flowing through temperate and tropical regions. Suitable dimensionless metrics are defined to characterize morphometric properties of meanders in terms of the spatio-temporal distribution of curvature and channel width. Results show the absence of marked contrasts in the amplitude of bend-curvature between the two data set. Differently, we find a permafrost signature in the channel width response, which manifests itself through larger values of the average bend-width and by peaks of width fluctuations. Field data suggest that permafrost meanders tend to widen for increasing bend sinuosity, likely promoting a shift of their morphodynamic regime as final cutoff is approached.

**Plain Language Summary** One of the most striking impacts of climate warming in the Arctic region is permafrost thaw. Arctic rivers typically flow through perennially-frozen floodplains, thus they are particularly susceptible to ground thawing. In order to understand the response of Arctic rivers to climate variability, basic knowledge about key differences with respect to non-permafrost streams is needed. Despite recent studies which have emphasized the slower yearly movement rates distinguishing Arctic streams, we still do not understand whether permafrost-affected rivers show distinctive features in their morphology due to specific physical mechanisms. By exploiting satellite imagery, we show that permafrost leaves a signature in the shape of meandering Arctic rivers. Specifically, their average bend-width increases as sinuosity develops, while the amplitude of width oscillations is larger than that displayed by their non-permafrost kin.

## 1. Introduction

Looking at an Arctic landscape is like looking at a painting. Rivers represent the warp of a canvas strewn with morphological features intimately tied to the presence of permafrost, as thermokarst lakes. Like their lower latitude kindred, northern streams manifest themselves across a continuum of patterns ranging from the two poles of multi-thread braiding and single-thread meandering. Here the attention is devoted to the latter family, namely meandering rivers carving their path through permafrost floodplains.

So far, our understanding of meandering rivers has been mainly restricted to streams located in temperate and tropical regions (Figure 1a). However, due to the raising awareness of the detrimental effects caused by the changing climate a growing attention has recently been paid to the behavior of fluvial systems in the Arctic (Figure 1b). Among the several implications related to atmospheric warming, the alteration of air and water temperatures are expected to accelerate river banks erosion causing an increasing amount of sediment loaded to streams (Rowland et al., 2010; Zhang et al., 2022). As a consequence, Arctic communities are threatened by several combined risks associated with permafrost thaw, such as increased flooding, accelerated bank recession, and damage of infrastructures (Hjort et al., 2018; Smith et al., 2022). Yet, there is still a poor understanding of the morphodynamics of Arctic streams, which hinders our comprehension of their potential geomorphic response to climate variability. In particular, it is still not clear whether there is a morphological signature embedded in the planform of rivers flowing through permafrost floodplains. But why should we expect some differences between the dynamics of permafrost and lower latitudes streams?

For decades, the dynamics of meandering streams has been primarily characterized in terms of curvature-driven effects on bed and channel planform development. However, meanders tend to display, to a certain degree, spatial and temporal oscillations of the channel width correlated with channel curvature (Eke, Czapiga, et al., 2014;

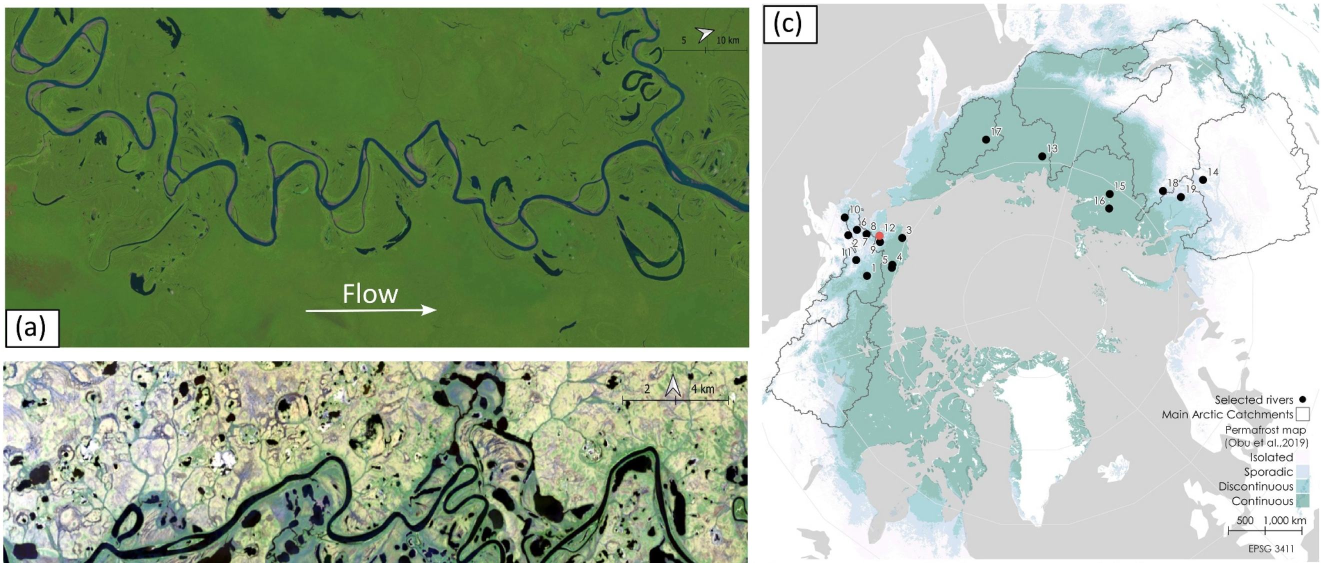


| ID | River | ID | River | ID | River |
|---|---|---|---|---|---|
| 1 | Porcupine, Alaska | 7 | Koyukuk #1, Alaska | 13 | Omoloj, Russia |
| 2 | Kuskokwim #1, Alaska | 8 | Kuoyukuk #2, Alaska | 14 | Vach, Russia |
| 3 | Unknown river #3, Alaska | 9 | Kobuk, Alaska | 15 | Unknown river #2, Russia |
| 4 | Iktilik, Alaska | 10 | Kuskokwim #2, Alaska | 16 | Unknown river #3, Russia |
| 5 | Kuparuk, Alaska | 11 | Tanana, Alaska | 17 | Kolyma, Russia |
| 6 | Innoko, Alaska | 12 | Selawick, Alaska | 18 | Yenisei, Russia |
| | | | | 19 | Taz, Russia |

**Figure 1.** Examples of typical non-permafrost and permafrost meandering streams with an overview of the investigated study reaches in the Arctic. On the left panels, Landsat images of meandering rivers: (a) Ucayali River, Perù, 5°40′S 74°18′W; (b) the Arctic Selawik River, Alaska (USA), 66°57′N 149°49′W. (c) Permafrost map based on Obu et al. (2019), in which the selected permafrost rivers are highlighted. The red dot indicates the Selawik River.

Frascati & Lanzoni, 2013; Luchi et al., 2010; Monegaglia et al., 2019; Seminara, 2006). As firstly observed by Brice (1975, 1982), the degree of morphological activity of meandering streams depends on the spatial distribution of channel width variations. The so-called *wider-at-bends* meanders, in which the widest cross-section is located close to the bend apex (Monegaglia et al., 2019), are found to be characterized by the highest rate of dynamism, while more stable configurations are observed in streams displaying a rather irregular width distribution. Wider-at-bends patterns appear to be dominated by bank processes (Zolezzi et al., 2012), in which different rates of migration of the advancing and retreating banks are forcing temporal variations of the channel width at the bend apex, where the outer retreating bank migrates faster than the inner one. Eventually, riparian vegetation can colonize the inner bank by encroachment (Asahi et al., 2013; Eke, Parker, & Shimizu, 2014; Perucca et al., 2007), and lately give rise to new portions of the floodplain (Zen et al., 2016). On the other hand, in-channel processes occurring in the central flow region are likely to play an important role in promoting local widening close to inflection points due to nonlinear curvature-width interactions (Luchi et al., 2011; Monegaglia et al., 2019; Zolezzi et al., 2012).

In Arctic environments, the winding movement is affected by further, unique, mechanisms that are strictly connected with the frozen floodplains through which rivers flow. Three main interrelated factors can be identified. First, channel migration can be controlled both by thermal and mechanical processes. Thermal processes lead to pore-ice melting, which is the primary responsible for the formation of peculiar morphological features like thermo-erosional niches or localized bank collapse due to thermal denudation (e.g., Costard et al., 2003; Douglas et al., 2023; Kanevskiy et al., 2016; Lawson, 1983; Walker & Hudson, 2003). Second, the hydrological regime, and consequently the sediment supply, is strongly seasonal. Most of the morphological activity occurs concurrently with ice break-up in spring and late summer floods (e.g., Scott, 1978; Tananaev & Lotsari, 2022; Walker et al., 1987; Walvoord & Kurylyk, 2016). Third, vegetation may have a weaker role in providing bank cohesion. The roots depth is limited by a seasonally-thawed active layer (e.g., Rowland et al., 2023), thus causing bank stability be mostly controlled by ice content and water temperature (Chassiot et al., 2020). It is reasonable to expect that these three major factors can affect planform morphologies, especially in contexts where bank erosion is primarily controlled by thermal processes (Douglas et al., 2023).

Existing studies mostly investigated the relationship between permafrost and non-permafrost rivers in terms of the absolute pace of lateral migration, and how ice-bounded streams are expected to respond to climate warming (Brown et al., 2020; Crampton, 1979; Ielpi et al., 2023; Rowland et al., 2023). The combination of both field measurements and satellite imagery showed the general tendency of Arctic rivers to migrate slower than non-permafrost streams. Thus, these studies essentially identified permafrost streams as a "slowly migrating version" of lower latitudes rivers. Yet, there is no evidence so far that the pace itself is really informative about the role of permafrost on the morphodynamic processes determining rivers dynamics. As suggested by standard meandering theories (e.g., Seminara, 2006; Seminara et al., 2001), if the timescale of planform development, which is proportional to the product of the erosion rate times the curvature, is properly re-scaled, even rivers with lateral migration rates of different order of magnitudes can show the same evolutionary behavior.

Here, the dynamics of permafrost meanders is investigated hypothesizing that their planform should be a manifestation of the distinctive physical processes they are shaped by. This hypothesis brings with it a basic question: what does distinguish the planform shape of a river carving its path into perennially-frozen ground compared to one which does not? In particular, is there some hallmark in the local values of planform parameters (width, curvature) of permafrost streams? To answer these questions, we compiled a data set of several permafrost sinuous rivers in the Arctic, which was later compared with an independent data set of non-permafrost rivers. As described in the next section, and more in detail in Supporting Information S1, the riverine active channels were extracted from multispectral Landsat images using Google Earth Engine over a temporal window of approximately 40 years. Successively, active channels were analyzed with the process-based software PyRIS (Monegaglia et al., 2018). The data were then investigated in terms of dimensionless metrics thus making it possible to rule-out possible scaling effects and reducing the subjectivity intrinsic in building the data set.

## 2. Methods

Arctic environments present multiple challenges mostly linked to ice-cover seasonality and the limited time window of the morphological activity. Furthermore, permafrost landscapes are characterized by a variety of small scale and medium scale features - among others, thermokarst lakes, scattered vegetation, bare soil areas, and mudboils - whose spatial variability affects negatively the detection of fluvial features from medium-resolution images, thus implying a greater remote sensing computational effort compared to non-permafrost environments. These issues were addressed by considering a set of meandering rivers bounded by frozen floodplains in the Arctic. Data collection spans over zones of continuous, discontinuous, and sporadic permafrost distribution on the basis of the map proposed by Obu et al. (2019) (Figure 1c). The extraction of permafrost meandering rivers was based on multispectral medium-resolution image filtering and segmentation, combining the cloud computing capability of Google Earth Engine (GEE) and PyRIS, a process-based tool for riverine multitemporal planform analysis (Monegaglia et al., 2018). Rivers were selected on the basis of: (a) their size, wider than approximately 100 m; (b) remote locations, where human disturbance is as far as possible minimized; (c) well-defined floodplains by avoiding confined reaches.

Considering that the typical Arctic climate leads to the absence of significant morphological activity during most of the year, we selected a time window that spans from May to September of each year to generate a single representative seasonal image. For each permafrost case, river mask pre-processing was performed on Landsat surface reflectance products (Landsat 5 Thematic Mapper, Landsat 7 Enhanced Thematic Mapper, Landsat 8 OLI/TIRS Collection 2). The implemented procedure combines synthetic representative multispectral indexes and anisotropic image filtering to improve the extraction of riverine active channels. As a result, the data set counts on 19 river reaches of the North American and Russian Arctic regions (see Tables S1–S2 in Supporting Information S1), for a total of 54 useable river masks from 1985 to 2021. The non-permafrost rivers data set contains 23 river reaches derived from a data set summarized in Tables S3–S4 in Supporting Information S1. To validate the limited spatial resolution of Landsat images, a subset of the narrower permafrost streams were compared with Sentinel-2 derived river masks showing a satisfactory agreement (see Figure S4 in Supporting Information S1).

The data set extracted with PyRIS in terms of binary masks include the longitudinal and transversal coordinates of the channel centerline (both in the UTM reference system and in the local reference system of the mask), the channel half-width, the inflection angle, and the channel curvature. Furthermore, the data set includes migration data, namely the longitudinal and lateral components of the migration vectors along with their magnitude, at least for the subset of the lumped data set for which the extraction was possible. Further details of the GEE and PyRIS

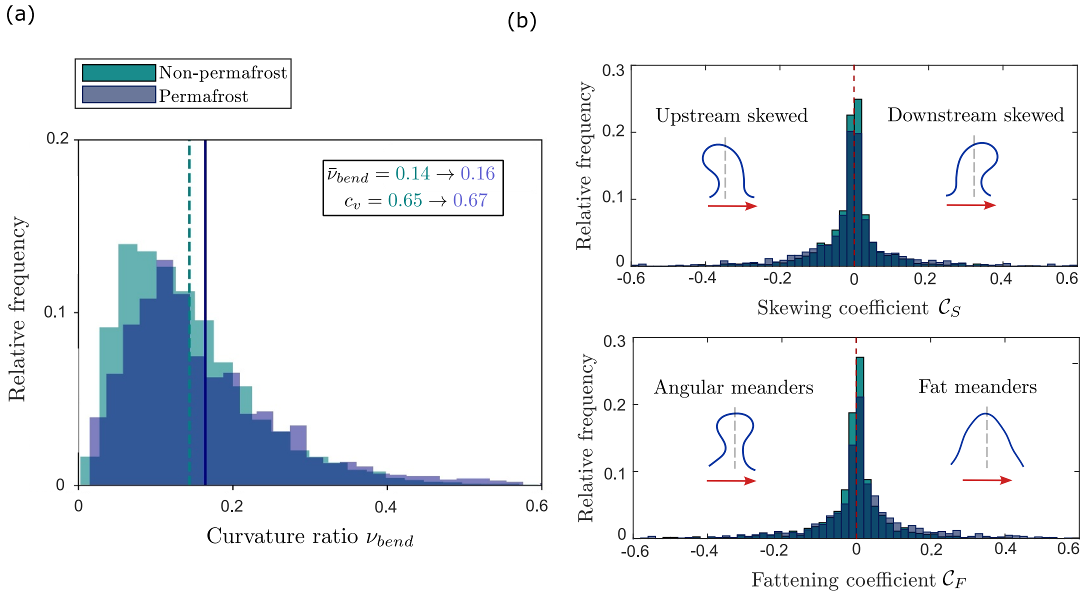


**Figure 2.** Comparison between non-permafrost and permafrost sinuous streams in terms of bend-curvature variations. (a) Relative frequency of the dimensionless bend curvature ($\nu_{bend}$). The vertical lines indicate the mean value ($\bar{\nu}_{bend}$), with $c_v$ the coefficient of variation (i.e., the ratio between the standard deviation and the mean). (b) Distribution of bend skewing ($C_S$) and fattening ($C_F$) coefficients for non-permafrost (teal bins) and permafrost (blue bins) rivers, respectively. The red arrow indicates flow direction. The null hyphothesis is verified by means of a Kolmogorov-Smirnov test at a significance level $p < 0.05$.

methodology are presented in *Supporting Information* (Texts S1–S2 in Supporting Information S1). The complete data set extracted with PyRIS can be found in Bonanomi et al. (2024a).

## 3. Results and Discussion

The evidence of permafrost-signatures in the morphometric properties of Arctic meanders is first sought by analyzing the overall spatio-temporal distribution of channel curvature through the dimensionless parameter $\nu$:

$$\nu = \frac{\overline{W}}{2R_r}, \tag{1}$$

with $R_r$ a characteristic value of the radius of curvature (here set as twice the radius of curvature at the bend apex), and $\overline{W}$ the average channel bend-width value. For both data set, the dimensionless curvature, as computed with reference to individual bends ($\nu_{bend}$, Figure 2a), displays a magnitude lower than unity, which is comparable with earlier findings on temperate and tropical rivers (e.g., Lagasse et al., 2004; Luchi et al., 2011; Monegaglia et al., 2019). When the two subset are analyzed separately, no significant differences are exhibited by the distributions, with mean values of 0.14 and 0.16 for non-permafrost and permafrost meanders, respectively.

The lack of a marked contrast in curvature variations can be further assessed by analyzing the extracted channel centerlines in terms of the widely employed simplified description of meander shape originally proposed by Kinoshita (1961):

$$C = 2\nu[\cos(\lambda_m s) - C_S \sin(3\lambda_m s) - C_F \cos(3\lambda_m s)], \tag{2}$$

where $C$ is the dimensionless curvature, $\lambda_m$ the intrinsic meander wavenumber, and $s$ the longitudinal coordinate measured along the centerline. The coefficients $C_S$ and $C_F$ account for bend skewing and fattening, respectively, and are obtained through a Continuous Wavelet Transform of the curvature signal following the method proposed by Vermeulen et al. (2016). With reference to the corresponding coefficients $\mathcal{S}$ and $\mathcal{F}$ as defined by Parker et al. (1983), $C_S$ and $C_F$ are given by:

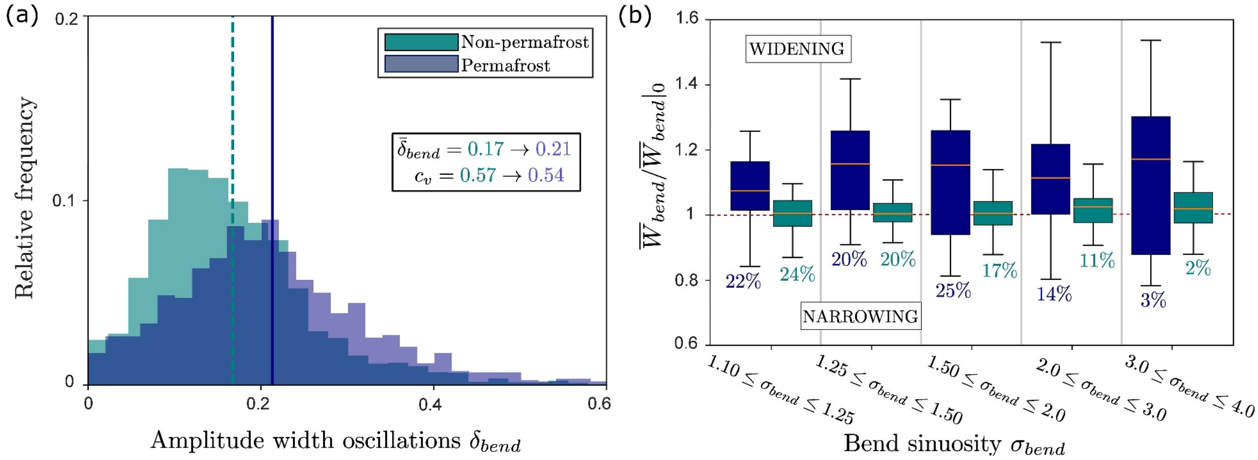


**Figure 3.** Comparison between non-permafrost and permafrost sinuous streams in terms of width variations. (a) Relative frequency of the magnitude of bend-width oscillations ($\delta_{bend}$). The vertical lines indicate the mean value $(\bar{\delta}_{bend})$, with $c_v$ the coefficient of variation. (b) Mean bend-width $(\overline{W}_{bend})$ normalized with the "low sinuosity" value $(\overline{W}_{bend}|_0)$ for permafrost (blue bins) and non-permafrost (teal bins) rivers. Data are shown for different sinuosity classes. The upper and lower limits of boxes correspond to the lower and upper quartile data values. For each sinuosity class, the percentage of bends within the whole subset is shown. The null hypothesis is verified by means of a Kolmogorov-Smirnov test at a significance level $p < 0.05$.

$$C_S = 3\mathcal{S}\theta_0^2, \qquad C_F = 3\mathcal{F}\theta_0^2, \tag{3}$$

with $\theta_0$ the amplitude of the inflection angle.

According with the definitions (Equation 3), a positive (negative) $C_S$ corresponds to downstream (upstream) skewed meanders. Likewise, positive (negative) $C_F$ coincides with fat (angular) meanders (Vermeulen et al., 2016). The results portrayed in Figure 2b show that both families of data almost split in two halves, where most meanders are found to be weakly skewed and fat. In general, a remarkable consistency is observed between the permafrost and non-permafrost distributions of planform coefficients. Figure 2 suggests that the degree of fattening and skewing is apparently weakly controlled by physical factors that are exclusively characteristics of Arctic watersheds, at least in the nearly-pristine meandering rivers with well-defined floodplains considered herein. We note that, through the sign of $C_S$, bend skewing can be interpreted as a proxy of the morphodynamic regime of the reach. Specifically, it has been shown theoretically that upstream (downstream) skewing occurs when the channel width-to-depth ratio is lower (higher) than a *resonant value* (Seminara et al., 2001; Zolezzi & Seminara, 2001), the latter being a function of the reach-averaged characteristics. Resonance defines the threshold between prevailing downstream or upstream influence of two-dimensional morphodynamic changes that are triggered by geometrical disturbances as channel curvature or width oscillations. Besides the first-order control that is exerted by in-stream channel morphodynamics on the planform evolution of river meanders, other factors may concur to determine the bend shapes, in particular those associated with floodplain heterogeneities (e.g., Güneralp & Rhoads, 2011). This notwithstanding, as also found by Guo et al. (2019), our analysis suggests that in reaches including dozens of bends, upstream (i.e., sub-resonant) and downstream-skewed (i.e., super-resonant) bends are found with roughly equal occurrence.

Having shown that channel curvature as a standalone indicator does not provide evidence of any significant permafrost-fingerprint, the planform geometry is then explored in terms of channel width variations. For this purpose, the dimensionless parameter $\delta$ quantifying the amplitude of width oscillations is defined as:

$$\delta = \frac{W_{\max} - \overline{W}}{2\overline{W}}, \tag{4}$$

with $W_{\max}$ the maximum bend-width value. In contrast with curvature variations, the permafrost data set shows a marked bias toward larger values of width oscillations at the bend scale $\delta_{bend}$ (Figure 3a), with a distribution that is statistically less skewed (i.e., more symmetric) with respect to the non-permafrost data set. The mean value passes from 0.17 to 0.21, which means that widest sections are appreciably wider than those of non-permafrost meanders. Nevertheless, values of $\delta_{bend}$ keep again well-below unity.

A clear and statistically significant difference between the two data set is also observed by analyzing the bend-averaged width $\left(\overline{W}_{bend}\right)$ as a function of the local sinuosity (i.e., the ratio between the intrinsic bend length and the Cartesian distance between the two subsequent inflection points, $\sigma_{bend}$). This is shown in Figure 3b, where $\overline{W}_{bend}$ is scaled by the "quasi-straight", "low-sinuosity" value $\overline{W}_{bend}|_0$, here set as the bend-averaged width corresponding to $1.0 \leq \sigma_{bend} \leq 1.1$. Indeed, since bend sinuosity tends to increase monotonically in time between meander formation and the final cutoff (Monegaglia et al., 2019; Seminara et al., 2001), $\sigma_{bend}$ can be used as a proxy of each bend's evolutionary stage (Monegaglia & Tubino, 2019). While data of non-permafrost rivers show a general tendency of the bend-averaged width to keep nearly constant, permafrost meanders display a gradual widening as bend elongates. Specifically, for values of $\sigma_{bend}$ typical of "mature meanders", the median value of $\overline{W}_{bend}$ exhibits a 20% increase with respect to the "young" initial stage.

A possible explanation for the observed difference in channel width response lies in the distinctive mechanisms driving the planform evolution of permafrost-affected meanders. The more pronounced width variations exhibited by Arctic rivers are symptomatic of larger differential migration rates between the eroding and the accreting bank. Since the period of morphological activity is constrained by seasonality, it is plausible that permafrost rivers have not enough time before the frozen period to enable the advancing inner bank to keep up with the retreating outer bank. In non-permafrost rivers it has been shown how width variations are positively correlated with the rate of chute cutoffs (Constantine et al., 2010; Zolezzi et al., 2012), with a higher frequency of wider-at-bends meanders when high sediment loads are available (Constantine et al., 2014). This observation might appear in contradiction with the considerably lower yearly sediment loads measured in Arctic rivers as compared to those located in lower latitudes (Gordeev, 2006). However, despite the fact that average annual bank erosion rates are usually smaller in rivers with permafrost (Figure S2 in Supporting Information S1, but see also Rowland et al. (2023)), previous studies highlighted how most of the sediment transport, and thus of the morphological activity, is concentrated within few weeks through the year (Walker et al., 1987; Walker & Hudson, 2003), potentially generating short-term, rapid and faster erosion rates (Costard et al., 2003; Douglas et al., 2023; Kanevskiy et al., 2016). Furthermore, bank erosion can be reinforced during spring floods by thaw-limited conditions (Douglas et al., 2023), whereby frozen sediment is eroded mainly through ablation (e.g., Costard et al., 2003; Kanevskiy et al., 2016; Lawson, 1983; Walker & Hudson, 2003). In contrast, the binding of sediment due to riparian vegetation is constrained by the resistance of trees and shrub to abrasion and ice-induced scours applied by drifting ice blocks (e.g., Ettema, 2008; Turcotte et al., 2011), by the short root depth with respect to bank height, and by the brief available time for vegetation to develop. All these effects could cause vegetation to have a lowered effectiveness on bank stability with respect to non-permafrost streams (Chassiot et al., 2020). Thus, permafrost streams are inferred to be prone to generating wider-at-bends meanders characterized by significant width oscillations (Figure S3 in Supporting Information S1).

Finally, the tendency of permafrost meanders to widen as long as they grow (Figure 3b) suggests that permafrost streams may be characterized by a shift of their morphodynamic regime from sub-resonant to super-resonant as the bends get more sinuous. It is worth noticing that previous theory of meandering (Monegaglia et al., 2019) showed that super-resonant meanders are particularly susceptible to width oscillations driven by curvature dynamics, which are associated with the formation of mid-channel bars (Hooke, 1986; Luchi et al., 2010). The net resulting picture is that permafrost meanders could be particularly inclined to develop transitional morphologies (Zolezzi et al., 2012), where features of both meandering and braiding patterns coexist along the same reach. How this transitional tendency may be affected by warmer temperatures is set as a goalposts for future investigations.

## 4. Conclusions and Perspectives

Recalling the key questions driving the present work, we can conclude that a permafrost signature manifests itself through channel width adjustments, specifically in the form of a progressive widening of the average bend-width, and of larger peaks of width oscillations. Thus, the peculiar physical conditions related with an Arctic environment, that is, the different variability of flow and thermal regime, sediment supply, the characteristics of riparian vegetation and the soil properties of the permafrost floodplains, are likely to promote the formation of wider-at-bends meanders characterized by wider cross-sections as bend sinuosity develops. As highlighted by various studies on river meandering (e.g., Monegaglia et al., 2019), such increase of the average channel width may lead permafrost meanders to become particularly sensitive to width oscillations generated by in-channel processes, and therefore to morphodynamic feedbacks between curvature and width oscillations, which are fundamentally nonlinear. Disentangling the in-stream and bank-driven contributions from remotely sensed data of the channel shape is anything but an easy task. However, satellite observations can be integrated with morphodynamic theories and analytical modeling, where one can take advantage of perturbation techniques by noting that, even in permafrost rivers, the dimensionless metrics quantifying curvature and width changes are both small quantities. In practice, this strategy would require extending the bend-scale theoretical framework of Monegaglia et al. (2019) to account for either the in-stream dynamics and the different rates of lateral shift of the channel banklines, and then coupling it with the recent reach-scale analysis by Monegaglia and Tubino (2019) that allows to compute the reach-averaged hydraulic properties of evolving meandering rivers.

## Conflict of Interest

The authors declare no conflicts of interest relevant to this study.

## Data Availability Statement

The complete GEE Python code, along with a demo river, is available at https://doi.org/10.5281/zenodo.10837177 (Crivellaro et al., 2024). PyRIS is freely available for download at https://doi.org/10.5281/zenodo.10837156 (Bonanomi et al., 2024b). The entire data set used for the analysis is publicly available at https://zenodo.org/records/10837907 (Bonanomi et al., 2024a).

**Acknowledgments**

This work has been carried out within the projects "SEDMORNET" funded by the European Union Next-GenerationEU (Piano Nazionale di Ripresa e Resilienza PNRR)—Mission 4—Component C2—Investment Fund 1.1 "Fondo per il Programma Nazionale di Ricerca e Progetti di Rilevante Interesse Nazionale (PRIN)", and the project DICAM-EXC (Departments of Excellence, 2023–2027, Grant L232/2016). The work has benefited from the comments of Kieran Dunne and one anonymous reviewer. The authors acknowledge Federico Monegaglia for having kindly shared the unpublished data set of non-permafrost rivers employed in the present analysis. Also the valuable suggestions and fruitful discussions with Marina Amadori, Alfonso Vitti and Guido Zolezzi are gratefully acknowledged. Open access publishing facilitated by Universita degli Studi di Trento, as part of the Wiley - CRUI-CARE agreement.

## References

Asahi, K., Shimizu, Y., Nelson, J., & Parker, G. (2013). Numerical simulation of river meandering with self-evolving banks. *Journal of Geophysical Research: Earth Surface*, *118*(4), 2208–2229. https://doi.org/10.1002/jgrf.20150

Bonanomi, R., Crivellaro, M., Ragno, N., Monegaglia, F., & Tubino, M. (2024a). Permafrost signature dataset [Dataset]. *Zenodo*. https://doi.org/10.5281/zenodo.10837907

Bonanomi, R., Crivellaro, M., Ragno, N., Monegaglia, F., & Tubino, M. (2024b). PyRIS v3.2.0 - Python RIvers by Satellite (v3.2.0) [Software]. *Zenodo*. https://doi.org/10.5281/zenodo.10837156

Brice, J. C. (1975). *Airphoto interpretation of the form and behavior of alluvial rivers (Tech. Rep.)*. Washington University, St. Louis: U.S. Army Research Office.

Brice, J. C. (1982). *Stream channel stability assessment (Tech. Rep.)*. Washington University, St. Louis: U.S. Federal Highway Administration. (Issue: January).

Brown, D. R., Brinkman, T. J., Bolton, W. R., Brown, C. L., Cold, H. S., Hollingsworth, T. N., & Verbyla, D. L. (2020). Implications of climate variability and changing seasonal hydrology for subarctic riverbank erosion. *Climatic Change*, *162*(2), 1–20. https://doi.org/10.1007/s10584-020-02748-9

Chassiot, L., Lajeunesse, P., & Bernier, J. F. (2020). Riverbank erosion in cold environments: Review and outlook. *Earth-Science Reviews*, *207*(September 2019), 103231. https://doi.org/10.1016/j.earscirev.2020.103231

Constantine, J. A., Dunne, T., Ahmed, J., Legleiter, C., & Lazarus, E. D. (2014). Sediment supply as a driver of river meandering and floodplain evolution in the Amazon Basin. *Nature Geoscience*, *7*(12), 899–903. https://doi.org/10.1038/ngeo2282

Constantine, J. A., McLean, S. R., & Dunne, T. (2010). A mechanism of chute cutoff along large meandering rivers with uniform floodplain topography. *Bulletin of the Geological Society of America*, *122*(5–6), 855–869. https://doi.org/10.1130/B26560.1

Costard, F., Dupeyrat, L., Gautier, E., & Carey-Gailhardis, E. (2003). Fluvial thermal erosion investigations along a rapidly eroding river bank: Application to the Lena River (Central Siberia). *Earth Surface Processes and Landforms*, *28*(12), 1349–1359. https://doi.org/10.1002/esp.592

Crampton, C. B. (1979). Changes in permafrost distribution produced by a migrating river meander in the northern Yukon, Canada. *Arctic*, *32*(2), 148–151. https://doi.org/10.14430/arctic2613

Crivellaro, M., Bonanomi, R., Ragno, N., Vitti, A., & Tubino, M. (2024). Google Earth Engine procedure for fluvial active channel semi-authomatic extraction on permafrost environment [Software]. *Zenodo*. https://doi.org/10.5281/zenodo.10837177

Douglas, M. M., Dunne, K. B. J., & Lamb, M. P. (2023). Sediment entrainment and slump blocks limit permafrost riverbank erosion. *Geophysical Research Letters*, *50*(11), e2023GL102974. https://doi.org/10.1029/2023GL102974

Eke, E. C., Czapiga, M. J., Viparelli, E., Shimizu, Y., Imran, J., Sun, T., & Parker, G. (2014). Coevolution of width and sinuosity in meandering rivers. *Journal of Fluid Mechanics*, *760*(September), 127–174. https://doi.org/10.1017/jfm.2014.556

Eke, E. C., Parker, G., & Shimizu, Y. (2014). Numerical modeling of erosional and depositional bank processes in migrating river bends with self-formed width: Morphodynamics of bar push and bank pull. *Journal of Geophysical Research: Earth Surface*, *119*(7), 1455–1483. https://doi.org/10.1002/2013JF003020

Ettema, R. (2008). Ice effects on sediment transport in rivers. In M. H. Garcia (Ed.), *Sedimentation engineering* (pp. 613–648). ASCE. https://doi.org/10.1061/9780784408148.ch13

Frascati, A., & Lanzoni, S. (2013). A mathematical model for meandering rivers with varying width. *Journal of Geophysical Research: Earth Surface*, *118*(3), 1641–1657. https://doi.org/10.1002/jgrf.20084

Gordeev, V. V. (2006). Fluvial sediment flux to the Arctic Ocean. *Geomorphology*, *80*(1–2), 94–104. https://doi.org/10.1016/j.geomorph.2005.09.008

Güneralp, n., & Rhoads, B. L. (2011). Influence of floodplain erosional heterogeneity on planform complexity of meandering rivers. *Geophysical Research Letters*, *38*(14), 2–7. https://doi.org/10.1029/2011GL048134

Guo, X., Chen, D., & Parker, G. (2019). Flow directionality of pristine meandering rivers is embedded in the skewing of high-amplitude bends and neck cutoffs. *Proceedings of the National Academy of Sciences of the United States of America*, *116*(47), 23448–23454. https://doi.org/10.1073/pnas.1910874116

Hjort, J., Karjalainen, O., Aalto, J., Westermann, S., Romanovsky, V. E., Nelson, F. E., et al. (2018). Degrading permafrost puts Arctic infrastructure at risk by mid-century. *Nature Communications*, *9*(1), 5147. (Publisher: Springer US). https://doi.org/10.1038/s41467-018-07557-4

Hooke, J. M. (1986). The significance of mid-channel bars in an active meandering river. *Sedimentology*, *33*(6), 839–850. https://doi.org/10.1111/j.1365-3091.1986.tb00986.x

Ielpi, A., Lapotre, M. G., Finotello, A., & Roy-Léveillée, P. (2023). Large sinuous rivers are slowing down in a warming Arctic. *Nature Climate Change*, *13*(4), 375–381. https://doi.org/10.1038/s41558-023-01620-9

Kanevskiy, M., Shur, Y. L., Strauss, J., Jorgenson, M. T., Fortier, D., Stephani, E., & Vasiliev, A. (2016). Patterns and rates of riverbank erosion involving ice-rich permafrost (yedoma) in northern Alaska. *Geomorphology*, *253*(December 2015), 370–384. https://doi.org/10.1016/j.geomorph.2015.10.023

Kinoshita, R. (1961). Investigation of channel deformation in Ishikari river. (Tech. Rep.). *Tokyo: Natural Resources Division, Ministry of Science and Technology of Japan*.

Lagasse, P. F., Spitz, W. J., Zevenbergen, L. W., Zachmann, D. W., & Associates, O. A. (2004). Handbook for predicting stream meander migration and supporting software (Tech. Rep.). (Publication Title: NCHRP Report 533). National Cooperative Highway Research Program. https://doi.org/10.17226/23346

Lawson, D. E. (1983). *Erosion of perennially frozen streambanks (Tech. Rep.). Washinton. D.C*. US Army Corps of Engineers.

Luchi, R., Hooke, J. M., Zolezzi, G., & Bertoldi, W. (2010). Width variations and mid-channel bar inception in meanders: River Bollin (UK). *Geomorphology*, *119*(1–2), 1–8. https://doi.org/10.1016/j.geomorph.2010.01.010

Luchi, R., Zolezzi, G., & Tubino, M. (2011). Bend theory of river meanders with spatial width variations. *Journal of Fluid Mechanics*, *681*, 311–339. https://doi.org/10.1017/jfm.2011.200

Monegaglia, F., & Tubino, M. (2019). The hydraulic geometry of evolving meandering rivers. *Journal of Geophysical Research: Earth Surface*, *124*(11), 2723–2748. https://doi.org/10.1029/2019JF005309

Monegaglia, F., Tubino, M., & Zolezzi, G. (2019). Interaction between curvature-driven width oscillations and channel curvature in evolving meander bends. *Journal of Fluid Mechanics*, *876*, 985–1017. https://doi.org/10.1017/jfm.2019.574

Monegaglia, F., Zolezzi, G., Güneralp, I., Henshaw, A. J., & Tubino, M. (2018). Automated extraction of meandering river morphodynamics from multitemporal remotely sensed data. *Environmental Modelling & Software*, *105*, 171–186. https://doi.org/10.1016/j.envsoft.2018.03.028

Obu, J., Westermann, S., Bartsch, A., Berdnikov, N., Christiansen, H. H., Dashtseren, A., et al. (2019). Northern Hemisphere permafrost map based on TTOP modelling for 2000–2016 at 1 km2 scale. *Earth-Science Reviews*, *193*(October 2018), 299–316. https://doi.org/10.1016/j.earscirev.2019.04.023

Parker, G., Diplas, P., & Akiyama, J. (1983). Meander bends of high amplitude. *Journal of Hydraulic Engineering*, *109*(10), 1323–1337. https://doi.org/10.1061/(asce)0733-9429(1983)109:10(1323)

Perucca, E., Camporeale, C., & Ridolfi, L. (2007). Significance of the riparian vegetation dynamics on meandering river morphodynamics. *Water Resources Research*, *43*(3), 1–10. https://doi.org/10.1029/2006WR005234

Rowland, J. C., Jones, C. E., Altmann, G., Bryan, R., Crosby, B. T., Geernaert, G. L., et al. (2010). Arctic landscapes in transition: Responses to thawing permafrost. *EOS Trans. AGU*, *91*(26), 229–230. https://doi.org/10.1029/2010EO260001

Rowland, J. C., Schwenk, J. P., Shelef, E., Muss, J., Ahrens, D., Stauffer, S., et al. (2023). Scale-dependent influence of permafrost on riverbank erosion rates. *Journal of Geophysical Research: Earth Surface*, *128*(7), e2023JF007101. https://doi.org/10.1029/2023JF007101

Scott, K. M. (1978). Effects of permafrost on stream channel behavior in Arctic Alaska. *U. S. Geological Survey Professional Paper*, *1068*, 1–19.

Seminara, G. (2006). Meanders. *Journal of Fluid Mechanics*, *554*(-1), 271–297. https://doi.org/10.1017/S0022112006008925

Seminara, G., Zolezzi, G., Tubino, M., & Zardi, D. (2001). Downstream and upstream influence in river meandering. Part 2. Planimetric development. *Journal of Fluid Mechanics*, *438*, 213–230. https://doi.org/10.1017/S002211200100427X

Smith, S. L., O'Neill, H. B., Isaksen, K., Noetzli, J., & Romanovsky, V. E. (2022). The changing thermal state of permafrost. *Nature Reviews Earth & Environment*, *3*(1), 10–23. https://doi.org/10.1038/s43017-021-00240-1

Tananaev, N. I., & Lotsari, E. (2022). Defrosting northern catchments: Fluvial effects of permafrost degradation. *Earth-Science Reviews*, *228*, 103996. https://doi.org/10.1016/j.earscirev.2022.103996

Turcotte, B., Morse, B., Bergeron, N. E., & Roy, A. G. (2011). Sediment transport in ice-affected rivers. *Journal of Hydrology*, *409*(1–2), 561–577. https://doi.org/10.1016/j.jhydrol.2011.08.009

Vermeulen, B., Hoitink, A. J. F., Zolezzi, G., Abad, J. D., & Aalto, R. E. (2016). Multiscale structure of meanders. *Geophysical Research Letters*, *43*(7), 3288–3297. https://doi.org/10.1002/2016GL068238

Walker, J. H., Arnborg, L., & Peippo, J. (1987). Riverbank erosion in the Colville delta, Alaska. *Geografiska Annaler—Series A: Physical Geography*, *69*(1), 61–70. https://doi.org/10.1080/04353676.1987.11880197

Walker, J. H., & Hudson, P. F. (2003). Hydrologic and geomorphic processes in the Colville River delta, Alaska. *Geomorphology*, *56*(3–4), 291–303. https://doi.org/10.1016/S0169-555X(03)00157-0

Walvoord, M. A., & Kurylyk, B. L. (2016). Hydrologic impacts of thawing permafrost-A review. *Vadose Zone Journal*, *15*(6), 1–20. https://doi.org/10.2136/vzj2016.01.0010

Zen, S., Zolezzi, G., Toffolon, M., & Gurnell, A. M. (2016). Biomorphodynamic modelling of inner bank advance in migrating meander bends. *Advances in Water Resources*, *93*, 166–181. https://doi.org/10.1016/j.advwatres.2015.11.017

Zhang, T., Li, D., East, A. E., Walling, D. E., Lane, S., Overeem, I., et al. (2022). Warming-driven erosion and sediment transport in cold regions. *Nature Reviews Earth & Environment*, *3*(12), 832–851. https://doi.org/10.1038/s43017-022-00362-0

Zolezzi, G., Luchi, R., & Tubino, M. (2012). Modelling morphodynamic processes in meandering rivers with spatial width variations. *Reviews of Geophysics*, *50*(4), 1–22. https://doi.org/10.1029/2012RG000392

Zolezzi, G., & Seminara, G. (2001). Downstream and upstream influence in river meandering. Part 1. General theory and application to overdeepening. *Journal of Fluid Mechanics*, *438*(13), 183–211. https://doi.org/10.1017/S0022112001004281

## References From the Supporting Information

Bertoldi, W., Drake, N. A., & Gurnell, A. M. (2011). Interactions between river flows and colonizing vegetation on a braided river: Exploring spatial and temporal dynamics in riparian vegetation cover using satellite data. *Earth Surface Processes and Landforms*, *36*(11), 1474–1486. https://doi.org/10.1002/esp.2166

Foga, S., Scaramuzza, P. L., Guo, S., Zhu, Z., Dilley, R. D., Beckmann, T., et al. (2017). Cloud detection algorithm comparison and validation for operational landsat data products. *Remote Sensing of Environment*, *194*, 379–390. https://doi.org/10.1016/j.rse.2017.03.026

Otsu, N. (1979). A threshold selection method from gray-level histograms. *IEEE Transactions on Systems, Man, and Cybernetics*, *C*(1), 62–66. https://doi.org/10.1109/TSMC.1979.4310076

Perona, P., & Malik, J. (1990). Scale-space and edge detection using anisotropic diffusion. *IEEE Transactions on Pattern Analysis and Machine Intelligence*, *12*(7), 629–639. https://doi.org/10.1109/34.56205

Rowland, J. C., Shelef, E., Pope, P. A., Muss, J., Gangodagamage, C., Brumby, S. P., & Wilson, C. J. (2016). A morphology independent methodology for quantifying planview river change and characteristics from remotely sensed imagery. *Remote Sensing of Environment*, *184*, 212–228. https://doi.org/10.1016/j.rse.2016.07.005

Spada, D., Molinari, P., Bertoldi, W., Vitti, A., & Zolezzi, G. (2018). Multi-temporal image analysis for fluvial morphological characterization with application to Albanian rivers. *ISPRS International Journal of Geo-Information*, *7*(8), 314. https://doi.org/10.3390/ijgi7080314